NeuroImage 47 (2009) 273–280

Contents lists available at ScienceDirect

NeuroImage

journal homepage: www.elsevier.com/locate/ynimg

Two temporal channels in human V1 identified using fMRI

Hiroshi Horiguchi [a,b,*], Satoshi Nakadomari [b,c], Masaya Misaki [d,e], Brian A. Wandell [a]

[a] Psychology Department, Stanford University, Stanford, CA 94305-2130, USA
[b] Department of Ophthalmology, Jikei University, School of Medicine, Tokyo, Japan
[c] Department of Functional Training III, National Rehabilitation Center for Persons with Disabilities, Tokorozawa, Japan
[d] Kobe Advanced ICT Research Center, National Institute of Information and Communications Technology, Japan
[e] Section on Functional Imaging Methods, Laboratory of Brain and Cognition, National Institute of Mental Health, National Institute of Health, USA

ARTICLE INFO

Article history:
Received 17 December 2008
Revised 25 March 2009
Accepted 27 March 2009
Available online 8 April 2009

Keywords:
fMRI
Temporal channel
V1
Luminance
Uniform

ABSTRACT

Human visual sensitivity to a fairly broad class of dynamic stimuli can be modeled accurately using two temporal channels. Here, we analyze fMRI measurements of the temporal step response to spatially uniform stimuli to estimate these channels in human primary visual cortex (V1). In agreement with the psychophysical literature, the V1 fMRI temporal responses are modeled accurately as a mixture of two (transient and sustained) channels. We derive estimates of the relative contributions from these two channels at a range of eccentricities. We find that all portions of V1 contain a significant transient response. The central visual field representation includes a significant sustained response, but the amplitude of the sustained channel signal declines with eccentricity. The sustained signals may reflect the emphasis on pattern recognition and color in the central visual field; the dominant transient response in the visual periphery may reflect responses in the human visual attention system.

Introduction

Time is nature's way of stopping everything from happening at once {attributed to John Wheeler}. Consequently, neurons in visual cortex must encode time-varying signals for many important visual functions, such as motion estimation. Psychophysical measurements suggest that the visual system measures temporal variations using a small number, but at least two, of temporal channels (Watson and Robson, 1981; Thompson, 1983; Hess and Plant, 1985). One channel is a relatively low-pass (sustained) temporal channel and the other channels are high-frequency, band-bass (transient) channels. Psychophysical assessments show further that the relative contribution of these channels to perception varies across visual field eccentricity; transient responses dominate in the periphery (McKee and Taylor, 1984; Snowden and Hess, 1992).

The temporal responses of neurons in the lateral geniculate nucleus and V1 support the psychophysical inference that the visual system contains only a small number of temporal channels. For example, De Valois and Cottaris (1998) explain the temporal responses of V1 cells by a linear combination of two temporal components. In addition, functional magnetic resonance imaging (fMRI) measurements in human extrastriate cortex show that different temporal channels contribute differentially to the responses in dorsal and ventral field maps. Neurons with higher temporal frequency responsivity dominate in dorsal and lateral extrastriate regions that compute motion, while lower temporal frequency responses dominate in ventral regions that are essential for object recognition and color perception (Liu and Wandell, 2005).

Within human V1, the signals from the different temporal channels appear to be interleaved at the scale of a typical fMRI voxel (e.g., 2 mm isotropic). Here, we develop an analysis to estimate the responses from these temporal channels, inter-mixed at sub-voxel resolution, in human visual cortex. Following the psychophysical and physiological results, we model the temporal receptive fields of transient and sustained neural channels. We derive the relative contributions from these channels from the BOLD response. We find that the relative contribution of the transient and sustained channels varies across the V1 visual field map. All portions of V1 contain a significant transient response. Signals near the foveal representation include a significant sustained temporal response, but the amplitude of the sustained channel signal declines with eccentricity. Hence, the relative significance of transient signals is higher in the periphery.

Materials and methods

Subjects

Five male subjects between the ages of 29 and 47 years participated in this study. All subjects had normal visual fields and normal or corrected-to-normal visual acuity. We dilated subjects'

* Corresponding author. Psychology, Stanford University, Jordan Hall, Building 420, Stanford, CA 94305-2130, USA.
E-mail address: hiroshih@stanford.edu (H. Horiguchi).

1053-8119/$ – see front matter © 2009 Elsevier Inc. All rights reserved.
doi:10.1016/j.neuroimage.2009.03.078

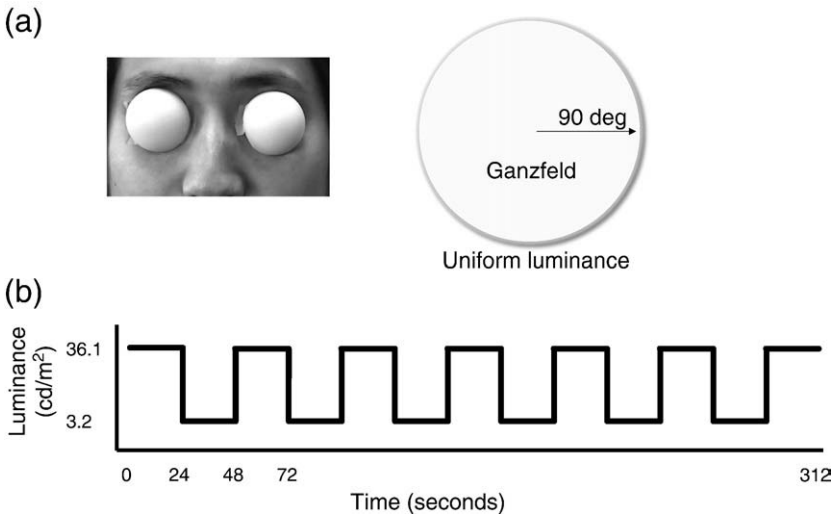

Fig. 1. Stimulus. (a) We placed semi-transparent hemisphere diffusers on both eyes (Ganzfeld). We also dilated subjects' pupils with mydriatics to maintain the pupil apertures at a constant size. All subjects experienced a uniform luminance without spatial contrast while the diffusers were illuminated. (b) Stimulus time series. The luminance followed a square wave (48 s period) alternation between 3.2 and 36.1 cd/m^2. There were six complete repetitions of the low–high luminance cycle as well as an initial 24 s period whose data were discarded (total scan time was 312 s).

pupils with mydriatics (Mydrin®-P ophthalmic solution; tropicamide and phenylephrine hydrochloride). This dilation prevents light reflex during the scan and thus avoids light-reflex contamination of the retinal illumination. All studies were performed with the informed written consent of subjects. All procedures adhered to protocols based upon the world medical association declaration of Helsinki ethical principles for medical research involving human subjects, approved by the ethical committees of National Institute of Information and Communications Technology.

Visual stimuli

The basic visual stimulus was a large, homogeneous field (Ganzfeld). To eliminate spatial contrast and obtain wide visual field in a narrow bore of MR scanner as much as possible, we placed semi-transparent, hemisphere-shaped diffusers over the subjects' eyes (Fig. 1a). The stimulus was a broadband light (achromatic, XYZ = 29.6, 36.1 cd/m^2, 29.9) from a projector (DLA-G150, Victor Company of Japan, Yokohama, Japan). The projector was imaged onto a front surface mirror at a 45 deg placed close to the subject's eyes. Subjects attempted to keep their direction of gaze constant, though with such a large uniform field stimulus some eye position drift is inevitable. When the luminance of the uniform field changed, the entire stimulus appeared to vary. There was no sense of differential brightening either near the fovea or near the surround.

The mean luminance of the field was modulated at a low temporal frequency square wave (1/24 Hz), effectively generating a series of step-on and step-off signals (Fig. 1b). The square wave illumination started with a 24 s exposure to a 36.1 cd/m^2. The luminance then alternated between 3.2 and 36.1 cd/m^2 every 24 s. The low–high luminance cycle was repeated 6 times during each scan (total scan time 312 s). Each subject completed 3 scans.

Stimuli were created and controlled using Visual Basic 6.0 (Microsoft Corp., Redmond, WA) and Direct X 7.0 (Microsoft) software programs on a personal computer (Windows XP, Microsoft).

Visual field map identification

In separate fMRI sessions we measured visual field maps using the traveling wave method (Engel et al., 1994, 1997). The stimuli consisted of high-contrast black and white dartboard patterns (temporal frequency, 4 Hz). Expanding rings and rotating wedges were used to estimate eccentricity and angular maps, respectively. The regions representing V1, V2 and V3 were identified using an atlas fitting algorithm (Dougherty et al., 2003). Regions of interest were created at various eccentricities of the V1 map on the horizontal meridian. Eccentricities at 5 and 10 deg could be determined from the maps. We extrapolated the maps to identify cortical locations representing 20, 40 and 60 deg from cortical magnification (Engel et al., 1997; Stenbacka and Vanni, 2007). We created a circular ROI with a 3 mm radius at each of these locations.

Task

To control attention, subjects were required to press a button every 2 s, synchronized with scanner noise.

Magnetic resonance imaging

FMRI data acquisition

The fMRI measurements were performed using a 3 T scanner with an 8 channel phased-array coil (Siemens Trio, Erlangen, Germany). Blood oxygenation level-dependent (BOLD) responses were acquired using 1-shot gradient-echo echo-planar imaging with the following settings: 25 planes; TR/TE 2000/36 ms ; flip angle, 90 deg; voxel size, 2 × 2 × 3 mm; fov, 192 mm. We chose axial slices parallel to the AC–PC line including the entire occipital lobe, recorded 156 imaging volumes, and discarded 12 volumes corresponding to the first 24 s.

Anatomical data acquisition

To classify the gray and white matter, we acquired whole-brain T1-weighted anatomical data (magnetization prepared rapid acquisition gradient-echo imaging sequence; 190 planes; TR/TE 9.7/4 ms ; flip angle, 12 deg; voxel size, 1 × 1 × 1 mm; fov, 256 mm; sagittal sections). Each fMRI session included acquisition of both functional and anatomical data in the same measurement planes (25 planes; TR/TE 580/17 ms ; flip angle, 55 deg; voxel size, 1 × 1 × 3 mm; acquisition order, interleave; averaging, 2; phase-partial Fourier, 7/8; fov, 192 mm).

Data processing

Anatomical processing. Gray and white matter regions were segmented from the anatomical MRI using custom software and hand-edited to

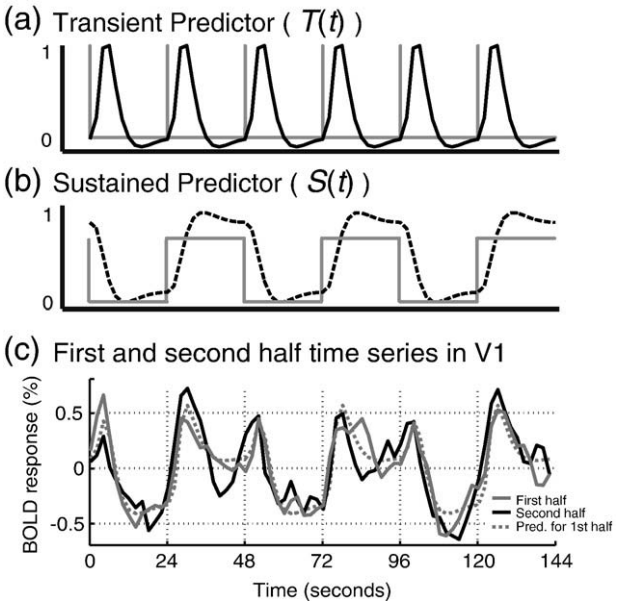

Fig. 2. Linear model predictors and their reliability. The gray-shaded lines show the (a) transient and (b) sustained models. The linear model predictors are calculated by convolving each model with the BOLD hemodynamic response, shown as the solid-black line (a) and the dashed-black line (b). (c) We compare three curves to assess data reliability and model precision: the first half of the averaged BOLD response in V1 across all hemispheres (gray-shaded line), the second half of this signal (black line), and a linear model estimate of the first half (dashed gray-shaded line). The linear model predicts the first half of the data about as well as the second half of the data predicts the first half.

minimize segmentation errors (Teo et al., 1997). The cortical surface was reconstructed at the white/gray matter border and rendered as a smoothed 3D surface (Wandell et al., 2000) (http://white.stanford.edu/software/).

Functional processing. The first 12 time-frames of each functional run were discarded due to start-up magnetization transients. Motion compensation for head movement within and between scans (Friston et al., 1995) was applied with Statistical Parametric Mapping (SPM) 2 software program (http://www.fil.ion.ucl.ac.uk/spm/software/spm2/). The drift in the time series mean level was removed by high-pass temporal filtering (f>0.025 Hz). Data were not spatially smoothed.

Model analysis. We created a linear model to predict the BOLD response to the square wave modulation of the Ganzfeld images (Fig. 2). The model-predictors were based on two temporal channels derived from psychophysical measurements (Watson and Robson, 1981; Thompson, 1983; Hess and Plant, 1985). Specifically, the psychophysical literature suggests that detection and discrimination of low spatial frequency patterns can be explained by a model comprising a sustained (low-pass) temporal channel and a transient (band-pass) channel. The temporal responses of these channels are very rapid compared to the slow hemodynamic response. Hence, the temporal impulse response function (tIRF) of the channels can be summarized by two linear predictors that represent (a) a transient response at onset and offset, and (b) a sustained response that tracks the stimulus luminance level. We model the transient response as positive at both onset and offset because previous fMRI studies show that both of increment and decrement of uniform surface luminance change evoked positive BOLD responses in visual cortex (Haynes et al., 2004; Boucard et al., 2005). By convolving the stimulus time course with the channel tIRF, we obtain the gray-shaded lines in Figs. 2ab. By further convolving these transient and sustained models with the BOLD hemodynamic response, we obtain the transient predictor (solid-black line, Fig. 2a) and the sustained predictor (dashed-black line Fig. 2b). The calculations used the default HRF function from the SPM 2 package, and we assumed the same HRF throughout V1. The BOLD response to the uniform stimulus differs very substantially across V1, far outside of the range that might be attributed to variation in the HRF.

We denote the transient and sustained predictors as $T(t)$ and $S(t)$ respectively. The linear model defines the relationship between the channel responses and the BOLD response, $y(t)$, as

$$y(t) = \beta_1 \cdot T(t) + \beta_2 \cdot S(t) + e$$

where β_1 and β_2 are scaling factors that account for the unknown units of the fMRI signal, and e is measurement noise. The $T(t)$ and $S(t)$ terms are nearly orthogonal ($r = -0.0138$). We estimated BOLD response for each estimated predictor by computing the β-coefficients to the time series at each voxel.

To verify the accuracy of the linear model we compare the linear model prediction with the stability of the data itself. The gray-shaded and black lines in Fig. 2c show the first and second half of the averaged BOLD response in the V1 representation between 2 and 10 deg, combined across all subjects. The dotted-gray line shows the linear model predictor to the first half of the data. The second half of the data predicts the first half well (data-to-data prediction), accounting for 67.9% of the variance (RMSE is 0.18). The two-dimensional model accounts for 86.4% of the variance (RMSE is 0.12), while the transient and sustained terms predict 44.7% and 41.6% of the variance, respectively. There is no reason to use a linear model with more than two terms because the two-dimensional model can explain the BOLD response better than the data-to-data prediction; there is no reason to use fewer than two terms because the individual predictors explain the BOLD less well than the data-to-data prediction.

Results

The response to temporal modulation of a uniform field is larger in V1 than extrastriate cortex

We plot the time course of BOLD responses from four regions of interest (Fig. 3). These regions span the 2–10 deg representations in V1, V2 and V3 and the confluent central representations of V1, V2 and

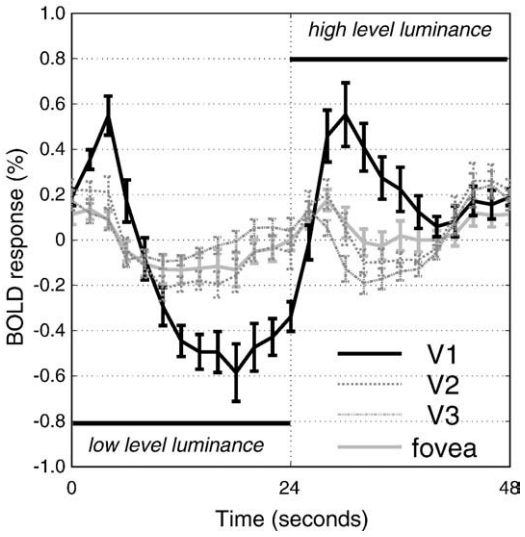

Fig. 3. BOLD responses in V1–V3. Each curve shows a single cycle of averaged BOLD response in V1, V2, V3 or the foveal confluence. Averaged BOLD responses in each visual field across all ten hemispheres and averaged across the six stimulus cycles are shown (error bar = ±1 SE.)

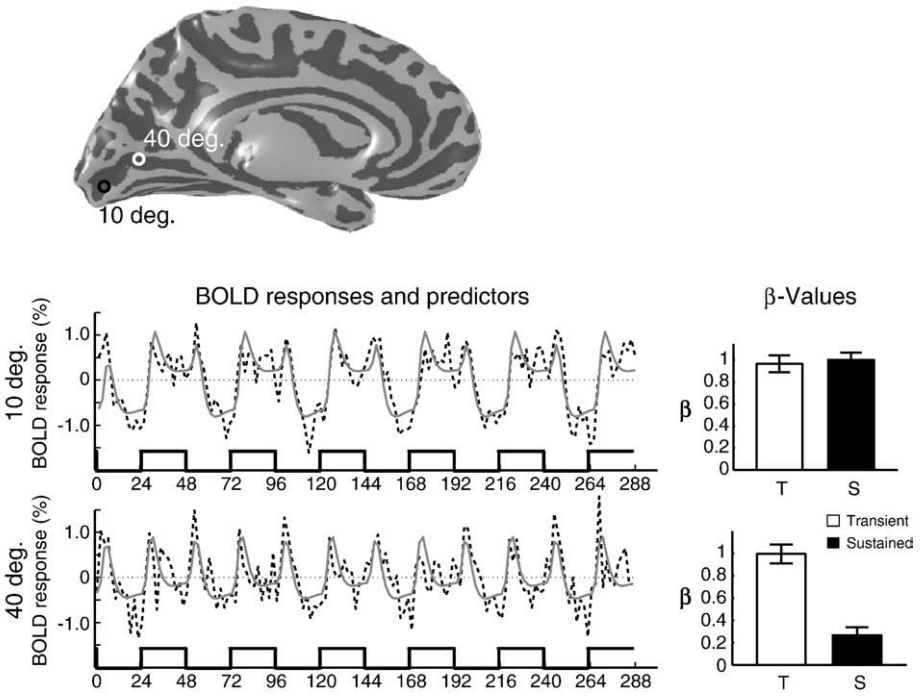

Fig. 4. Comparing BOLD responses and β-values within a typical subject. Averaged time series and β-values from ROIs in posterior and anterior V1 of a typical subject are plotted. The ROI positions are shown on the brain (inset upper left). These ROIs represent 10 deg (posterior, black circle) and 40 deg (anterior, white circle) eccentricities. At 10 deg eccentricity, the BOLD response (dashed-black line) is well-fit by the weighted sum of sustained and transient predictors (gray line). The β-values of both transient and sustained predictors were approximately equal. At 40 deg eccentricity the best fitted predictor for BOLD is more impulsive and predominantly fit by the transient predictor. The β-values are the average from all of the voxels within each ROI. The error bar is ±1 SE.

V3 (within the central 2 deg). Each time course is derived by averaging the responses to 18 dark–light alternations across three scan sessions and ten hemispheres (five subjects).

Notice three features of the responses. First, the V1 modulation is three times larger than the response in extrastriate regions. Second, the V1 BOLD response is lower when the luminance is lower. Third, there are two local peaks in the V1 response, one following light-offset and a second following light-onset. A linear model with the transient and sustained predictors explains over 80% of the variance in the V1 BOLD response averaged across all voxels and subjects. The stimulus-related modulations beyond V1 are either very small (V2) or below the noise level. The stimulus-driven linear model explains only 20% of the variance of the average V2 response and almost none of the variance in V3. We compared the consistency of V1 and V2 BOLD responses individually (Supplemental Fig. 1), and we find that only the V1 responses are consistent across subjects. Given that the BOLD response modulation is mainly confined to V1, the remaining analyses focus on that part of cortex.

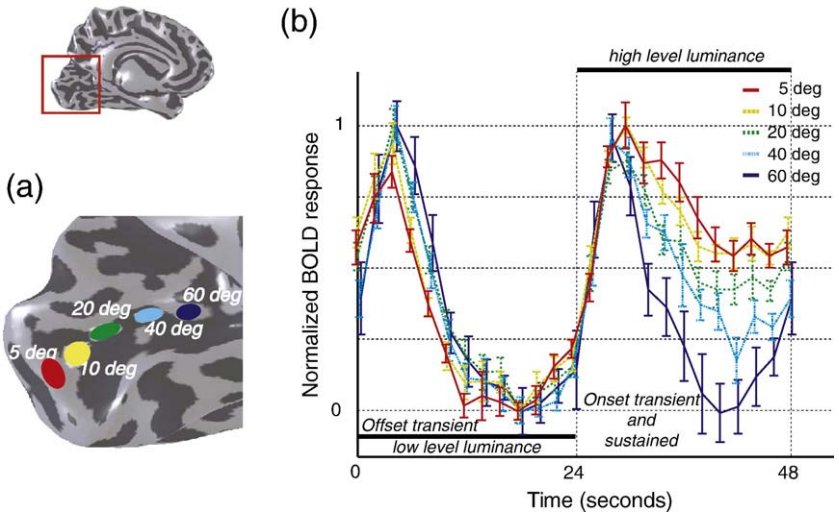

Fig. 5. Single cycle V1 BOLD responses from ROIs at different five eccentricities. (a) V1 regions of interest. Five circular ROIs (radius = 3 mm) were defined along the V1 horizontal meridian. The ROIs at 5 and 10 deg eccentricity could be determined from the maps. We set three ROIs with centers at 20, 40 and 60 deg eccentricity, respectively. (b) BOLD responses from ten hemispheres (five subjects) were averaged in each ROI defined in panel (a). To facilitate comparison of the modulations in these different ROIs, the responses were normalized between 0 and 1. Each color represents an ROI that responds best to a different eccentricity. Note the BOLD responses have two characteristic. First, across all eccentricities the responses have two peaks localized near the luminance offset and onset. These transients are the same during the luminance-offset time. Second, during the luminance-onset phase, the initial transient is the same at all eccentricities but the sustained response differs. Specifically, BOLD responses during light-onset phase gradually and systematically decrease with increasing eccentricity. (Error bar = ±1 SE.)

The balance between transient and sustained response in V1 varies with eccentricity

The average time series in the central and peripheral V1 visual field representations differ. The curves in Fig. 4 show responses in relatively posterior and anterior locations within calcarine cortex (10 and 40 deg eccentricities) in the left hemisphere of a typical subject. At 10 deg eccentricity, the BOLD response (dashed-black line) is well-fit by the weighted sum of two predictors (gray-shaded line). The transient (β_1) and sustained (β_2) predictors are approximately equal. At 40 deg eccentricity, the best fitted predictor is more impulsive and predominantly fit by the transient predictor.

The average BOLD time series at five V1 ROIs representing different eccentricities are shown in Fig. 5. These time series were averaged across 18 dark–light alternations, three scan sessions, and combined from ten hemispheres (five subjects). To facilitate comparison of the modulations in these different ROIs, the responses were normalized between 0 and 1 (see Supplemental Fig. 2 for the unnormalized data). The responses have two peaks localized near the luminance offset and onset. The transients at different eccentricities are the same during the luminance-offset phase. During the luminance-onset phase, the initial rise is the same at all eccentricities but the sustained response differs. Specifically, after the transient response the mean level remains higher at locations near the foveal representation but drops to zero for locations in the far periphery representation. Hence the foveal regions of V1 have both a transient and sustained response, while the peripheral representation is dominated by the transient response.

To quantify the contributions of the transient and sustained components, we applied linear model analysis voxel-by-voxel and measured the weights (β_1,β_2). The difference between these weights is shown by the color overlay on the inflated cortical surface of the posterior left hemisphere of a typical subject (Fig. 6a). To eliminate noisy voxels, the color overlay is shown only at those positions where the linear model explains at least 10% of the variance in the BOLD response and $\beta_1+\beta_2>0$.

For all subjects the relative contributions from the two linear predictors vary systematically from posterior to anterior calcarine sulcus. The relative weight of the sustained component exceeds the transient component weight in the foveal region. In the peripheral representation, the transient component dominates. In Supplemental Fig. 3 we show the data from all ten hemispheres. In Supplemental Fig. 4 we show additional analyses that support the hypothesis that the response becomes increasingly transient with increasing eccentricity.

Transient response amplitudes are similar across the visual field, but sustained amplitudes decrease with increasing eccentricity

We further quantified the relative contributions of the two predictors with increasing eccentricity in V1 (Fig. 6b). We calculate the contribution of each predictor in explaining the averaged BOLD response by normalizing the β-weight by the ratio of the predictor standard deviation and the BOLD response standard deviation (Cohen et al., 1983). This simply transforms the linear model so that the predictor vectors have equal vector length.

$$C_t = \beta_1 \cdot \frac{std(T(t))}{std(y(t))}$$

$$C_s = \beta_2 \cdot \frac{std(S(t))}{std(y(t))}$$

Each colored line shows the contribution of the predictor at different eccentricities for one subject. The transient predictor is approximately constant or slightly increasing across eccentricity, and the sustained predictor declines with eccentricity for all subjects.

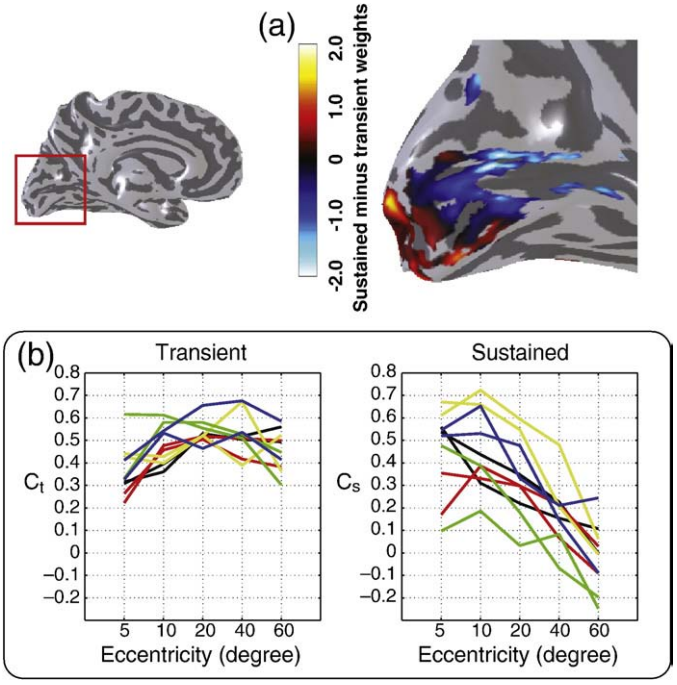

Fig. 6. Relative contribution between transient and sustained predictor. An inflated cortical surface of the left hemisphere of one subject (inset at upper left). The red box shows the position of the expanded region in Fig. 6a. (a) Pseudo-color map shows the difference between the transient and sustained predictor weights, (β_1,β_2). Negative values indicate dominant transient voxels (blues); positive values indicate dominant sustained voxels (orange, yellow). The relative contributions vary gradually and systematically from posterior to anterior calcarine. Overlay colors are only plotted when the variance-explained ≥10% and $\beta_1+\beta_2>0$. (b) Relative contribution of transient ($C(t)$) and sustained ($C(s)$) predictors. Each curve shows one subject. The transient weights are roughly constant across eccentricity, while the sustained weights decline with eccentricity.

Discussion

Psychophysical measurements of visual temporal sensitivity can be explained by models using two temporal channels (Watson and Robson, 1981; Thompson, 1983; Hess and Plant, 1985; Snowden and Hess, 1992). The BOLD measurements described here show that the V1 time series are also well-described by a two-dimensional linear model. Psychophysically derived channel tIRFs describe responses at a much finer time scale than can be measured using BOLD. Nonetheless, it is possible to derive BOLD response predictions using these channels and a simple model. Here, we show that there is an excellent quantitative agreement between the psychophysically estimated temporal channels and the BOLD responses in V1.

The model relating the neural and BOLD responses can be specified using the following formulae:

$$N(t) = \int S_i(t-r)I(r) + (T_i(t-r)I(r))^2 dr$$

$$B(t) = \int h(t-u)N(u)du$$

In this formula the BOLD response, B, is calculated by convolving the hemodynamic response function, $h()$, with the neural response, $N()$. The neural response is calculated as the sum of two terms. The first is the convolution of the sustained channel, $S_i()$ with the stimulus luminance, $I()$. The second term is the squared convolution of the luminance and transient channel impulse response function, $T_i()$. This term is squared because there is a positive BOLD response to both positive and negative transients.

We estimate the sustained, $S_i()$ and transient $T_i()$channels as weighted combinations of the psychophysical tIRFs (McKee and Taylor, 1984). Specifically, we calculate a weighted difference between the foveal and peripheral psychophysical tIRFs to estimate, $S_i()$. The weight is chosen so that the sustained channel has mostly positive tIRF. We calculate a second weighted difference between the foveal and peripheral tIRFs to estimate a transient channel, $T_i()$. In this case, the weight is chosen so that the transient channel has zero area under the curve. The sustained and transient tIRFs are shown in Fig. 7 (inset, upper left).

The two curves in Fig. 7a show the predicted BOLD response assuming equal sustained and transient components, as in the central field (gray line), or a predominantly transient component, as in the periphery (black line). At luminance offset there is a transient response in both near-fovea and periphery. The BOLD response then decays to a low value. At luminance onset, the near-fovea and periphery both respond transiently. Over time the peripheral response decays further because it has a lower sustained component. The measured V1 BOLD responses at 5 and 40 deg regions of interest are shown in Fig. 7b. These curves are from Fig. 5, and they represent the average responses from all ten hemispheres. The properties of the measurements agree quite well with the model predictions.

Neural basis of the signals

It is possible that the responses measured to these large uniform fields are confined to the small subset of the V1 cells known as 'Luxotonic cell' (Kayama et al., 1979) or 'Type-I neuron' (Kinoshita and Komatsu, 2001). These cells respond to zero spatial contrast stimuli within each receptive field and encode an absolute luminance-dependent response. If the number of Luxotonic cells that respond to luminance increments and decrements is balanced, then one might not expect any BOLD response to a uniform field. However, single unit population samples suggest that roughly four times as many Luxotonic cells respond to luminance increments compared to decrements. This is consistent with the observation that the BOLD response increases during the high luminance phase of the stimulation.

The neural temporal channels may be implemented in at least two different ways. As previously described, one hypothesis is that these channels reflect the responses of different classes of neurons, say the magnocellular and parvocellular pathways (Rodieck et al., 1985; Merigan and Maunsell, 1993; Wandell, 1995). The relative amplitudes of the BOLD responses do not match the spatial densities of these two retinal ganglion cell types (Dacey, 1993). However, we cannot rule out the hypothesis that there is a correspondence between these cell types and the transient and sustained responses; there may be a nonlinear relationship between the BOLD response amplitudes and the number of neurons (Mullen et al., 2008). An alternative hypothesis is that the biophysical parameters governing temporal responses change within all cell populations as we measure at different locations within the visual field. For example, Solomon et al. (2005) show that the sustained-transient balance changes even within a single retinal ganglion cell class.

Extending the model

A goal for this project is to build a simulation of V1 responses to a broad range of stimuli. In previous work, several groups have examined the spatial receptive fields of V1 neurons (Dumoulin and Wandell, 2008; Kay et al., 2008; Thirion et al., 2006). The experiments and analyses here extend that work to the temporal responses of large uniform fields. While we learned a great deal about the sustained and transient temporal responses from these simple stimuli, the stimulus set is very limited. The next set of measurements and analyses should test the model defined here by using stimuli that include a variety of temporal modulations, as well as stimuli with more complex spatial structures.

One simplification in the current measurements concerns the lack of response in extrastriate cortex (Supplemental Fig. 5). Because the

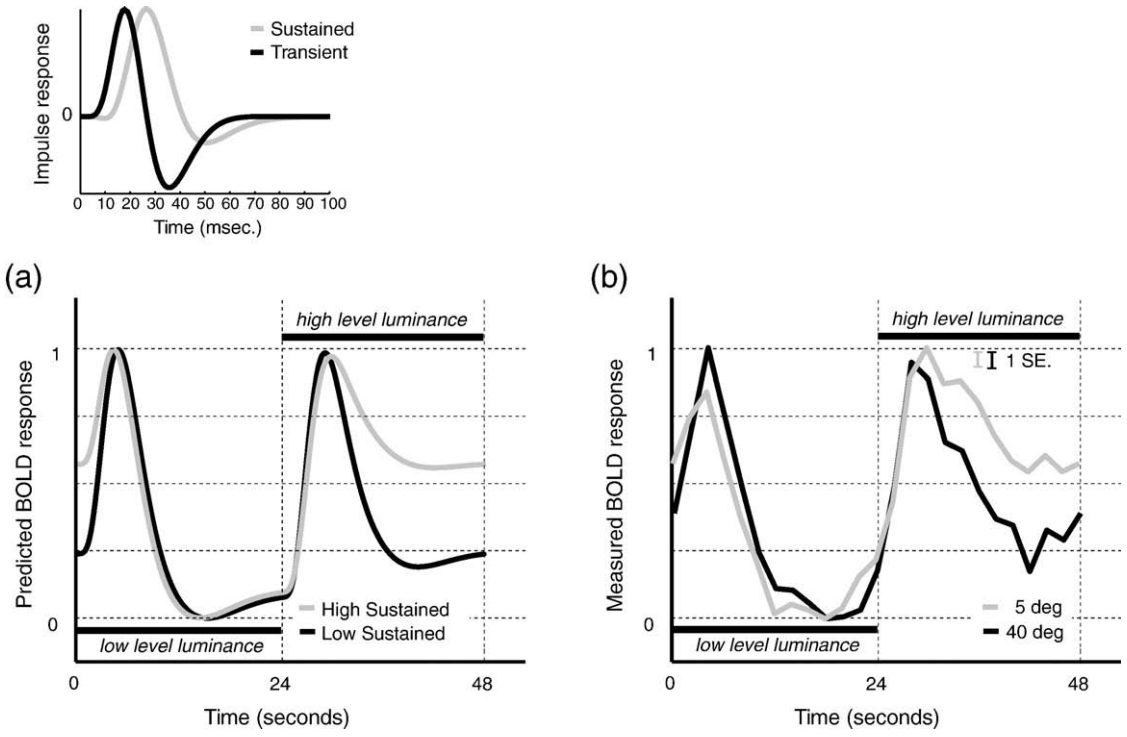

Fig. 7. Comparison of predicted and measured BOLD responses. (a) The predicted BOLD response in a region with predominantly transient (solid-black) or mixed sustained and transient (gray-shaded) regions. (b) BOLD responses from peripheral (40 deg, solid-black) and foveal (5 deg, gray-shaded) regions of V1. (Error bar = 1 SE for a typical point.) The inset (upper left) shows the transient and sustained channels derived from psychophysical data. See text for details of the model predictions.

Ganzfeld stimulus did not produce an extrastriate response there was probably no feedback from extrastriate cortex to V1. As we generalize the stimuli to include combined spatial and temporal contrast, we expect to find responses in extrastriate cortex. Future modeling may require additional complexity that accounts for these interactions.

General analyses of transient and sustained signals

In a recent study, Uludag (2008) considered whether transient components of the BOLD response, including the transient pre- and post-stimulus overshoots, are neuronal or vascular. In that work, subjects viewed a flickering stimulus presented to one hemifield. The author fit a linear model containing a transient and sustained regressor to the BOLD response. The transient regressor weight was significantly greater than zero even in ipsi-lateral LGN and visual cortex, despite the fact that the stimulus presentation was restricted to one hemifield. Unlike the present study, Uludag did not find transient responses in the foveal regions. The differences in stimulus and analysis methods are quite significant so that some BOLD response discrepancies might be expected. Uludag interpreted the transient responses as part of a neuronal attentional network, rather than a feature of the HRF. The data described here show that across several centimeters within V1 the balance of sustained and transient components shifts gradually. These measurements support Uludag's view that the sustained and transient responses have a neural, rather than vascular, origin.

Other papers report transient and sustained components of the BOLD responses in visual cortex (Chen et al., 1998; Uludag, 2008). That work differs from ours in several ways. First, it uses stimuli that include both spatial contrast and temporal flicker. Second, no measurements are analyzed systematically across visual field maps. Third, neither paper includes a model of the neural responses. Our findings integrate psychophysics and electrophysiology with a neural model. The work here represents a first step towards characterizing the temporal response properties of various neural populations in early visual cortex.

A combination of transient and sustained BOLD responses has been analyzed in other cortical systems, too. In auditory cortex, Harms et al. (2005) reported that simple manipulations of the auditory waveform alter the balance between sustained and transient BOLD responses in Heschl's (A1) and in the superior temporal gyrus. Fox et al. (2005) identify significant transient and sustained responses in a variety of tasks. Like Uludag, they argue that these transient responses have a neural, not vascular, origin. They further show that regions responding transiently will be overlooked by an analysis with only a sustained regressor. Finally, Burgund et al. (2006) report measuring both sustained and transient BOLD responses during a cognitive letter-judgment task. Interestingly, the developmental trajectories of the sustained and transient response components differ: the sustained component decreases and the transient component increases with age.

Conclusions

We used a model-based fMRI approach to identify temporal responses in visual cortex. The method used here extends the model-based spatial analysis (Dumoulin and Wandell, 2008) to temporal responses. Consistent with temporal psychophysical sensitivity, the fMRI data comprise two terms, a sustained and transient channel. The balance between the two temporal channels varies with eccentricity. Transient responses are constant or relatively increasing as one measures from fovea to periphery; sustained responses are mainly confined to the central visual representation. The sustained responses in the central visual field may be used to increase the signal-to-noise acquired about targets near the fovea. This may be useful for perceiving high spatial resolution and color. The emphasis on dynamic responses in the periphery is consistent with a visual system that uses dynamic peripheral stimuli to draw visual attention so that the stimulus can be analyzed using information derived from the high-resolution fovea.

Acknowledgment

We thank Jonathan Winawer, Serge O. Dumoulin, Kaoru Amano, Rory Sayres, Ayumu Furuta, Yoichiro Masuda, Kunihiro Asakawa, Kenji Kitahara, Hiroshi Tsuneoka, Shigeyuki Kan, Takahiko Koike, and Satoru Miyauchi for useful discussions. Supported by Grant-in-Aid for JSPS Fellows (20.11472) to HH, Grant-in-Aid for JSPS Fellows (18.164) to MM and NEI grant RO1-EY03164 to BW.

Appendix A. Supplementary data

Supplementary data associated with this article can be found, in the online version, at doi:10.1016/j.neuroimage.2009.03.078.

References

Boucard, C.C., van Es, J.J., Maguire, R.P., Cornelissen, F.W., 2005. Functional magnetic resonance imaging of brightness induction in the human visual cortex. Neuroreport 16, 1335–1338.
Burgund, E.D., Lugar, H.M., Miezin, F.M., Schlaggar, B.L., Petersen, S.E., 2006. The development of sustained and transient neural activity. Neuroimage 29, 812–821.
Chen, W., Zhu, X.H., Kato, T., Andersen, P., Ugurbil, K., 1998. Spatial and temporal differentiation of fMRI BOLD response in primary visual cortex of human brain during sustained visual simulation. Magn. Reson. Med. 39, 520–527.
Cohen, P., Cohen, J., West, S.G., Aiken, L.S., 1983. Applied multiple regression/correlation analysis for the behavioral sciences. Erlbaum, Hillsdale, NJ.
Dacey, D.M., 1993. The mosaic of midget ganglion cells in the human retina. J. Neurosci. 13, 5334–5355.
De Valois, R.L., Cottaris, N.P., 1998. Inputs to directionally selective simple cells in macaque striate cortex. Proc. Natl. Acad. Sci. U. S. A. 95, 14488–14493.
Dougherty, R.F., Koch, V.M., Brewer, A.A., Fischer, B., Modersitzki, J., Wandell, B.A., 2003. Visual field representations and locations of visual areas V1/2/3 in human visual cortex. J. Vis. 3, 586–598.
Dumoulin, S.O., Wandell, B.A., 2008. Population receptive field estimates in human visual cortex. Neuroimage 39, 647–660.
Engel, S.A., Rumelhart, D.E., Wandell, B.A., Lee, A.T., Glover, G.H., Chichilnisky, E.J., Shadlen, M.N., 1994. fMRI of human visual cortex. Nature 369, 525.
Engel, S.A., Glover, G.H., Wandell, B.A., 1997. Retinotopic organization in human visual cortex and the spatial precision of functional MRI. Cereb. Cortex 7, 181–192.
Fox, M.D., Snyder, A.Z., Barch, D.M., Gusnard, D.A., Raichle, M.E., 2005. Transient BOLD responses at block transitions. Neuroimage 28, 956–966.
Friston, K.J., Ashburner, J., Frith, C.D., Poline, J.B., Heather, J.D., Frackowiak, R.S.J., 1995. Spatial registration and normalization of images. Hum. Brain Mapp. 2, 165–189.
Harms, M.P., Guinan Jr., J.J., Sigalovsky, I.S., Melcher, J.R., 2005. Short-term sound temporal envelope characteristics determine multisecond time patterns of activity in human auditory cortex as shown by fMRI. J. Neurophysiol. 93, 210–222.
Haynes, J.D., Lotto, R.B., Rees, G., 2004. Responses of human visual cortex to uniform surfaces. Proc. Natl. Acad. Sci. U. S. A. 101, 4286–4291.
Hess, R.F., Plant, G.T., 1985. Temporal frequency discrimination in human vision: evidence for an additional mechanism in the low spatial and high temporal frequency region. Vision Res. 25, 1493–1500.
Kay, K.N., Naselaris, T., Prenger, R.J., Gallant, J.L., 2008. Identifying natural images from human brain activity. Nature 452, 352–355.
Kayama, Y., Riso, R.R., Bartlett, J.R., Doty, R.W., 1979. Luxotonic responses of units in macaque striate cortex. J. Neurophysiol. 42, 1495–1517.
Kinoshita, M., Komatsu, H., 2001. Neural representation of the luminance and brightness of a uniform surface in the macaque primary visual cortex. J. Neurophysiol. 86, 2559–2570.
Liu, J., Wandell, B.A., 2005. Specializations for chromatic and temporal signals in human visual cortex. J. Neurosci. 25, 3459–3468.
McKee, S.P., Taylor, D.G., 1984. Discrimination of time: comparison of foveal and peripheral sensitivity. J. Opt. Soc. Am. A 1, 620–627.
Merigan, W.H., Maunsell, J.H., 1993. How parallel are the primate visual pathways? Annu. Rev. Neurosci. 16, 369–402.
Mullen, K.T., Dumoulin, S.O., Hess, R.F., 2008. Color responses of the human lateral geniculate nucleus: selective amplification of S-cone signals between the lateral geniculate nucleno and primary visual cortex measured with high-field fMRI. Eur. J. Neurosci. 28, 1911–1923.
Rodieck, R.W., Binmoeller, K.F., Dineen, J., 1985. Parasol and midget ganglion cells of the human retina. J. Comp. Neurol. 233, 115–132.
Snowden, R.J., Hess, R.F., 1992. Temporal frequency filters in the human peripheral visual field. Vision Res. 32, 61–72.

Solomon, S.G., Lee, B.B., White, A.J., Ruttiger, L., Martin, P.R., 2005. Chromatic organization of ganglion cell receptive fields in the peripheral retina. J. Neurosci. 25, 4527–4539.
Stenbacka, L., Vanni, S., 2007. fMRI of peripheral visual field representation. Clin. Neurophysiol. 118, 1303–1314.
Teo, P.C., Sapiro, G., Wandell, B.A., 1997. Creating connected representations of cortical gray matter for functional MRI visualization. IEEE Trans. Med. Imag. 16, 852–863.
Thirion, B., Duchesnay, E., Hubbard, E., Dubois, J., Poline, J.B., Lebihan, D., Dehaene, S., 2006. Inverse retinotopy: inferring the visual content of images from brain activation patterns. Neuroimage 33, 1104–1116.
Thompson, P., 1983. Discrimination of moving gratings at and above detection threshold. Vision Res. 23, 1533–1538.
Uludag, K., 2008. Transient and sustained BOLD responses to sustained visual stimulation. Magn. Reson. Imaging 26, 863–869.
Wandell, B.A., 1995. Foundation of Vision. Sinauer, Sunderland, MA.
Wandell, B.A., Chial, S., Backus, B.T., 2000. Visualization and measurement of the cortical surface. J. Cogn. Neurosci. 12, 739–752.
Watson, A.B., Robson, J.G., 1981. Discrimination at threshold: labelled detectors in human vision. Vision Res 21, 1115–1122.